

# Relative Contribution of Central and Peripheral Aberrations to Overall High Order Corneal Wavefront Aberration

Marco Lombardo, MD; Giuseppe Lombardo, Eng, PhD; Michele Manzulli, MD; Marino Palombi, MD; Sebastiano Serrao, MD, PhD

## ABSTRACT

**PURPOSE:** To analyze the influence of specific combinations of corneal high order aberrations on the optical image quality of the cornea before and after photorefractive keratectomy (PRK) for low to high myopia and myopic astigmatism.

**METHODS:** Corneal topography was obtained for 80 eyes that underwent PRK using a scanning-spot excimer laser. The eyes were subdivided into three groups according to the preoperative refraction. The topographical data were imported into a custom software program that combined the Zernike high order terms having the same sign and angular frequency up to seventh order for 4-mm and 6-mm pupils, ie, coma and spherical aberrations, and midperipheral and peripheral high order aberrations.

**RESULTS:** Photorefractive keratectomy induced a significant amount of the root-mean-square (RMS) values of the combinations of midperipheral and peripheral high order aberrations over the smaller pupil size for deeper myopic ablations ( $P < .05$ ). Over the larger pupil, spherical myopic ablations showed a significant increase ( $P < .05$ ) of the RMS values of coma and spherical aberrations. In the astigmatism group, the combination of terms having higher angular frequency increased significantly ( $P < .05$ ) after surgery both over 4-mm and 6-mm pupils.

**CONCLUSIONS:** After surface ablation, ablation depth and profile significantly influence the distribution and contribution of determined combinations of high order aberrations to the overall high order corneal wavefront aberration. Terms having high angular frequency were increased following large myopic correction and wide treatment zone. Quality of the whole corneal optics will be enhanced by designing future ablation profiles to compensate for peripheral high order optical aberrations. [*J Refract Surg.* 2006;22:656-664.]

**W**avefront-guided customized ablation is an emerging technique in refractive surgery performed with the goal to minimize the whole eye optical aberrations. With the development of this technique, many authors are establishing aberration standards for normal individuals and the visual effects of each aberration to optimize the results of correction.<sup>1-5</sup>

Improvements in the technology and methodology of wavefront-guided laser ablation are expected to correct the variability in some individual factors<sup>6-8</sup> and thereby further optimize the quality of vision.<sup>9-12</sup> Besides the biophysical factors<sup>6</sup> that cannot be predicted by a wavefront approach and need to be further investigated to minimize unwanted changes of the cornea after refractive procedures, the assessment of the preoperative eye should take into account the interaction between aberrations and the effect of their combinations on vision function. The wide variability of high order aberrations of the eye in the healthy population and the complex combination of individual terms in modulating visual performance make it difficult to correctly treat the individual high order wavefront aberration to achieve a super-normal vision.<sup>4,13</sup>

Adaptive optics and the generation of aberrated acuity charts can reliably inform us on the combined effects of high order aberrations on the retinal image.<sup>14,15</sup> Applegate et al<sup>15</sup> stated the interaction between terms having the same sign and angular frequency (eg, 0, -2, or 2) may produce a combined effect on improving acuity if compared to the individual effect of each mode. Furthermore, it is known that for an equal amount of root-mean-square (RMS) error, each mode of Zernike expansion has a different impact on visual performance and that the Zernike modes concentrated near the cen-

*From Vision Engineering, Reggio Calabria, Italy (M. Lombardo); the Department of Physics, Excellence Center CEMIF.CAL, CNR-INFM Licryl Laboratory, University of Calabria, Rende (Cs), Italy (G. Lombardo); Serralaser, Rome, Italy (Manzulli, Serrao); and St John Hospital, Rome, Italy (Palombi).*

*The authors have no financial interest in the materials presented herein.*

*Correspondence: Marco Lombardo, MD, Via Adda 7, 00198 Rome, Italy. Tel/Fax: 39 06 8840971; E-mail: mflombardo@libero.it*

*Received: May 12, 2005*

*Accepted: February 22, 2006*

*Posted online: May 15, 2006*

ter of the pupil impact visual performance more than the combination of terms having a higher level of angular frequency.<sup>15-17</sup> However, much less attention has been directed to the contribution of peripheral high order aberrations of the visual optics on the visual performance.<sup>18</sup> The relative contribution of Zernike terms with higher angular frequency to the overall high order wavefront aberration may greatly increase over a dilated pupil,<sup>18,19</sup> especially after the larger ablation zone sizes commonly used today. This phenomenon could be exaggerated at relatively low levels of whole eye aberrations, which is the goal of wavefront-guided customized ablation, and therefore the effect of peripheral optical aberrations on vision may be underestimated.

The purpose of this investigation was to determine the weight and effect of combinations of Zernike modes near the edge of each radial order in affecting the optical image quality of the corneal first surface in comparison with specific combinations of central and paracentral high order aberrations in a population of myopic eyes before and 1 year after photorefractive keratectomy (PRK). The normalized Zernike expansion was used for specifying the corneal wavefront error and to decompose the wavefront error into individual error modes. In this study, corneal first surface high order terms having the same sign and angular frequency were combined based on previous literature.<sup>15-17,20</sup> The effect on optical image quality of the cornea was then visualized by computing the corneal point spread function (PSF).<sup>21</sup>

#### PATIENTS AND METHODS

This prospective, randomized study included 80 eyes in 40 patients (14 men and 26 women). Mean patient age was  $31.7 \pm 5.95$  years (range: 25 to 45 years). Eyes were divided into three groups based on preoperative refraction.<sup>22</sup> The low myopia group ( $-1.50$  to  $-4.50$  diopters [D]) consisted of 30 eyes (6 men and 9 women); the high myopia group ( $-4.60$  to  $-8.00$  D) consisted of 30 eyes (5 men and 10 women); and the astigmatism group ( $-2.00$  to  $-5.00$  D of myopic astigmatism with-the-rule and  $-0.25$  to  $-5.50$  D sphere) consisted of 20 eyes (3 men and 7 women). In the low myopia and high myopia groups, the cylinder component was  $\leq 1.00$  D.

Patients were considered eligible for the study if they were at least 21 years old, had no ocular disease and no previous ocular surgery, and had refractive stability for at least 2 years. Patients who used contact lenses were asked to stop wearing the lenses for at least 4 weeks prior to surgery. Informed consent was obtained from all patients. Institutional review board approval was not required for this study.

The corneal epithelium was removed using the Amoils' brush. The PRK procedure was performed using a Chiron Technolas Keracor 217C excimer laser (Bausch & Lomb, Dornach, Germany) with an ablation zone diameter of 6 mm and a transition zone up to 9 mm in diameter; an active eye tracker device was used. The astigmatism group was treated with a cross-cylinder technique<sup>23</sup> (photorefractive astigmatic keratectomy) with a 6-mm ablation zone diameter and a transition zone up to 9 mm in diameter. As described previously,<sup>24</sup> phototherapeutic keratectomy was performed (using a viscous-masking 0.25% sodium hyaluronate solution for a smoothing technique) at the end of the procedure. The smoothing technique proved to be more effective in inducing less high order aberrations than standard PRK.<sup>24</sup>

All patients underwent a complete ocular evaluation, including corneal topography and pupillometry (Keratron Scout; Optikon 2000, Rome, Italy). The topographer is equipped with a special lamp board placed behind the mires cone that illuminates the mires with either visible light or infrared to obtain pupil measurements in both photopic and mesopic light conditions. The follow-up protocol of this study included examinations preoperatively and 1 year postoperatively. For each eye, measurements were repeated five times to assess the repeatability of the topography.<sup>25</sup> Reproducibility and accuracy of videokeratoscopic measurements were tested using an artificial spherical cornea provided by the manufacturer and calculated from five independent measurements. The standard deviation for the high order RMS surface error of the sphere was  $\pm 0.007 \mu\text{m}$  and  $\pm 0.02 \mu\text{m}$  at 4 mm and 6 mm diameter, respectively.

The topographer software calculated the corneal wavefront aberration on the corneal elevation with respect to an ideal aspherical corneal shape with eccentricity  $1/n$  (where  $n=1.3375$ ); the wavefront aberration then was obtained from the derivatives using a least-squares best-fit<sup>26</sup> procedure and described as a seventh order Zernike polynomial expansion.<sup>27</sup> We then exported the aberration data output, computed with respect to the line of sight using the move axis function of the topographer and the photopic and mesopic pupil diameters from the topographer for analysis. Preoperative and 1-year postoperative corneal aberration data were computed for 4-mm and 6-mm pupils.<sup>28</sup> The smaller pupil size ensured that we analyzed the high order corneal wavefront aberration changes exclusively within the ablation zone, whereas the larger pupil size allowed us to calculate the high order corneal wavefront aberration in the scotopic condition. First and second orders were not considered. The Zernike polynomials were normal-

ized such that over the pupil, the RMS for each Zernike mode was unity.<sup>29</sup> The recommended Optical Society of America notation is used describing individual Zernike terms with a two-index scheme.<sup>30,31</sup>

Pre- and postoperative aberration data were processed using custom software written in MATLAB (software version 7.0) (MathWorks Inc, Natick, Mass). The parameters analyzed included: 1) the RMS of the spherical aberration (the square root of the sum of the squared coefficients of  $Z_4^0$  and  $Z_6^0$ ); 2) the RMS of coma (the square root of the sum of the squared coefficients of  $Z_3^{-1}$ ,  $Z_3^1$ ,  $Z_5^{-1}$ , and  $Z_5^1$ ); 3) the RMS of midperipheral high order aberrations (the square root of the sum of the squared coefficients  $Z_3^{-3}$ ,  $Z_3^3$ ,  $Z_4^{-2}$ ,  $Z_4^2$ ,  $Z_5^{-3}$ ,  $Z_5^3$ ,  $Z_6^{-2}$ ,  $Z_6^2$ ,  $Z_7^{-3}$ , and  $Z_7^3$ ); and 4) the RMS of peripheral high order aberrations (the square root of the sum of the squared coefficients  $Z_4^{-4}$ ,  $Z_4^4$ ,  $Z_5^{-5}$ ,  $Z_5^5$ ,  $Z_6^{-6}$ ,  $Z_6^6$ ,  $Z_7^{-7}$ ,  $Z_7^7$ , and  $Z_7^7$ ). The combinations of central and paracentral high order terms of the Zernike pyramid for analysis were chosen based on previous publications,<sup>15-17,20,32-34</sup> and the combinations of terms having higher angular frequency represented a subset of the possible combinations of higher order Zernike modes.<sup>16</sup> To assess the accuracy of this type of analysis, a vector approach has been applied to the Zernike representation of the wavefront error. Terms having single or higher angle symmetries were represented in the magnitude/axis method, as reported by Campbell<sup>35</sup> and also in the American National Standards Institute (ANSI) standard for reporting wavefront error (ANSI Z80.28-2004). The alignment of vector axes for each determined combination of terms having the same azimuthal index has been examined. For example, the mean angle of the vector axes created by combining functions having a single angle symmetry, such as  $Z_3^{-1}$  and  $Z_3^1$  as well as  $Z_5^{-1}$  and  $Z_5^1$ , was 12° and 8°, respectively, over the larger cornea area of analysis in our study population, showing the vectors were mostly aligned and therefore their vector sum can properly represent coma. Root-mean-square data were expressed as mean±standard deviation and measured in microns.

The terms used in this work to describe combinations of Zernike modes (ie, central or peripheral aberrations) are anatomically related to the pupil area analysis, representing different portions of the aberrant incident wavefront. For example, the peripheral or midperipheral aberrations represent the optical effect of high order aberrations on the edge of the area of analysis or close to it, respectively.

Because we aimed to characterize the visual effect of corneal high order aberrations in the scotopic condition, the software allowed us to obtain optical quality pupil maps by computing the corneal PSF for a 6-mm

pupil.<sup>36,37</sup> The PSF was calculated using the corneal wavefront data with the following formulas:

$$PSF = |FT(PF(x,y))|^2 \quad (A)$$

where FT is the 2D Fourier transform and PF is the pupil function. The pupil function PF has two components, an amplitude component  $A(x,y)$  and a phase component that contains the wave aberration  $W(x,y)$ . The amplitude component  $A(x,y)$  defines the shape, size, and transmission of the optical system and represents an attenuating factor. For  $A(x,y)$ , we used a *circ function* that defines a circular aperture of ray = 3.0 mm and transmission unitary inside the circ and zero outside:

$$PF(x,y) = A(x,y)e^{-i\frac{2\pi}{\lambda}W(x,y)} \quad (B)$$

where  $\lambda$  is the wavelength of light used (555 nm). The Stiles-Crawford effect, which is a different attenuation of the amplitude of the light distribution across the pupil  $A(x,y)$ , was not incorporated in our computation as it was outside the scope of this work (only the role of the anterior cornea on image quality was investigated).

The Wilcoxon signed rank test was performed to evaluate variations between preoperative and 1-year postoperative parameters in each study group. The Spearman rank correlation test was performed to analyze changes of determined combinations of Zernike modes independent of spherical equivalent and cylinder. The level of significance was .05 for all of the tests performed.

## RESULTS

Table 1 summarizes the pre- and postoperative mean spherical equivalent refraction for all of the study groups. The refractive target was emmetropia in all cases. All of the procedures were uneventful; after surgery, no eye lost one or more Snellen lines of spectacle-corrected visual acuity. The average photopic and mesopic pupil diameters were  $3.40 \pm 0.55$  mm and  $5.77 \pm 1.03$  mm, respectively, in the low myopia group;  $3.77 \pm 0.78$  mm and  $5.69 \pm 1.04$  mm, respectively, in the high myopia group; and  $3.41 \pm 0.38$  mm and  $5.55 \pm 0.75$  mm, respectively, in the astigmatism group.

The preoperative analysis of the high order aberrations showed absolute values that were highest for the coma terms in comparison with determined combinations of Zernike modes in all of the study groups over the smaller pupil size. Over a 6-mm pupil, wavefront analysis showed an increased value of the mean RMS value of each determined combination of high order aberrations compared to the 4-mm pupil size in all of the study groups.<sup>5,38</sup> Therefore, the preoperative analy-

TABLE 1  
**Mean ( $\pm$ SD) Preoperative and 1-year Postoperative Spherical Equivalent Refraction (D) for the Three Study Groups**

Group	Preoperative	Postoperative	P Value
Low myopia (range: -1.50 to -4.50 D) (n=30)	-3.04 $\pm$ 0.73	+0.003 $\pm$ 0.27	<.05
High myopia (range: -4.60 to -8.00 D) (n=30)	-5.91 $\pm$ 1.26	+0.07 $\pm$ 0.38	<.05
Astigmatism (range: -2.00 to -5.00 D cylinder) (range: -0.25 to -5.50 D sphere) (n=20)	-4.21 $\pm$ 2.42	-0.75 $\pm$ 0.83	<.05

TABLE 2  
**Mean ( $\pm$ SD) Preoperative and Postoperative Root-Mean-Square of High Order Aberrations ( $\mu$ m) in 4-mm and 6-mm Pupils for the Low Myopia Group**

	4-mm Pupil		6-mm Pupil	
	Preoperative	Postoperative	Preoperative	Postoperative
Coma	0.088 $\pm$ 0.043	0.124 $\pm$ 0.120	0.253 $\pm$ 0.112	0.337 $\pm$ 0.09*
Spherical aberration	0.058 $\pm$ 0.016	0.100 $\pm$ 0.098*	0.278 $\pm$ 0.054	0.388 $\pm$ 0.104*
Midperipheral high order aberrations	0.071 $\pm$ 0.026	0.070 $\pm$ 0.029	0.182 $\pm$ 0.075	0.198 $\pm$ 0.085
Peripheral high order aberrations	0.044 $\pm$ 0.015	0.052 $\pm$ 0.022	0.079 $\pm$ 0.030	0.098 $\pm$ 0.050

\*Statistically significant P<.05

TABLE 3  
**Mean ( $\pm$ SD) Preoperative and 1-year Postoperative Root-Mean-Square of High Order Aberrations ( $\mu$ m) in 4-mm and 6-mm Pupils for the High Myopia Group**

	4-mm Pupil		6-mm Pupil	
	Preoperative	Postoperative	Preoperative	Postoperative
Coma	0.081 $\pm$ 0.039	0.206 $\pm$ 0.192*	0.308 $\pm$ 0.176	0.449 $\pm$ 0.201*
Spherical aberration	0.074 $\pm$ 0.022	0.110 $\pm$ 0.026*	0.322 $\pm$ 0.093	0.694 $\pm$ 0.154*
Midperipheral high order aberrations	0.069 $\pm$ 0.024	0.111 $\pm$ 0.047*	0.195 $\pm$ 0.101	0.215 $\pm$ 0.191
Peripheral high order aberrations	0.057 $\pm$ 0.027	0.076 $\pm$ 0.034*	0.089 $\pm$ 0.034	0.135 $\pm$ 0.028

\*Statistically significant P<.05

sis of the high order RMS wavefront variance showed no distinction between the study groups, as reported previously,<sup>39</sup> except for slightly larger values in the astigmatism group in comparison with the simple myopia groups. Tables 2, 3, and 4 summarize the mean

RMS of determined combinations of high order aberrations for all of the study groups.

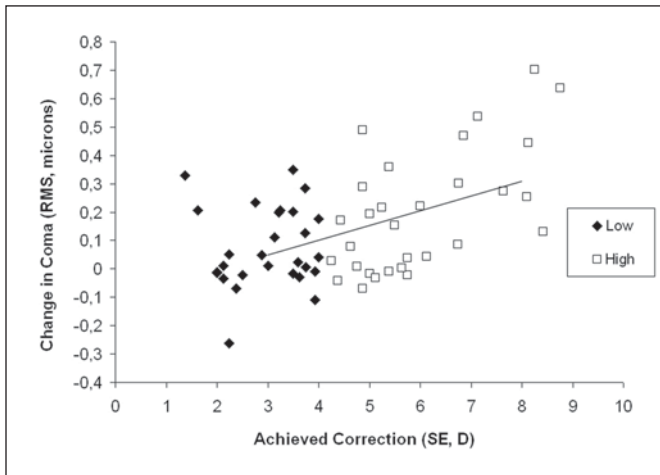
At the end of follow-up, with the exception of the astigmatism group, the mean RMS of coma and spherical aberration increased over a 4-mm pupil. In detail,

TABLE 4

**Mean ( $\pm$ SD) Preoperative and 1-year Postoperative Root-Mean-Square of High Order Aberrations ( $\mu$ m) in 4-mm and 6-mm Pupils for the Astigmatism Group**

	4-mm Pupil		6-mm Pupil	
	Preoperative	Postoperative	Preoperative	Postoperative
Coma	0.123 $\pm$ 0.042	0.112 $\pm$ 0.050	0.413 $\pm$ 0.118	0.427 $\pm$ 0.202
Spherical aberration	0.073 $\pm$ 0.016	0.057 $\pm$ 0.034	0.307 $\pm$ 0.044	0.298 $\pm$ 0.192
Midperipheral high order aberrations	0.083 $\pm$ 0.032	0.130 $\pm$ 0.041*	0.191 $\pm$ 0.079	0.435 $\pm$ 0.127*
Peripheral high order aberrations	0.040 $\pm$ 0.009	0.058 $\pm$ 0.020*	0.087 $\pm$ 0.032	0.147 $\pm$ 0.071*

\*Statistically significant  $P < .05$



**Figure 1.** Correlation scattergram between the achieved correction in spherical equivalent (SE) and the change in root-mean-square (RMS) values in coma over a 6-mm pupil in the low and high myopia groups (Spearman correlation coefficient  $R=0.42$ ,  $P < .01$ ). The solid line represents a linear fit to the data.

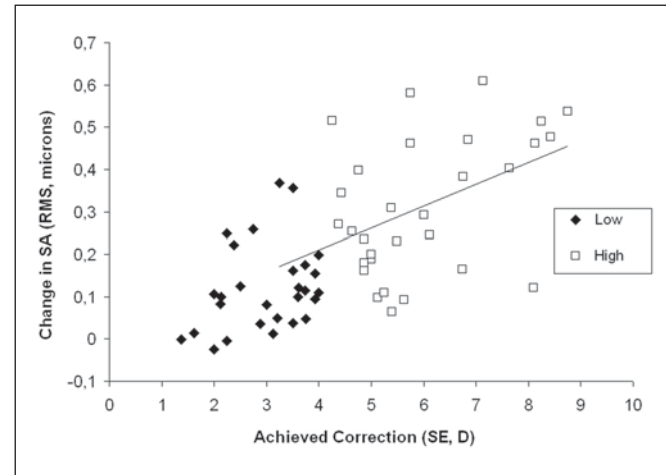


**Figure 2.** Correlation scattergram between the achieved correction in spherical equivalent (SE) and the change in root-mean-square (RMS) values in spherical aberration (SA) over a 6-mm pupil in the low and high myopia groups (Spearman correlation coefficient  $R=0.63$ ,  $P < .001$ ). The solid line represents a linear fit to the data.

the increase in the magnitude value of spherical aberration was significant in the low myopia group ( $P < .001$ ), and there was a statistically significant increase both for coma ( $P < .001$ ) and spherical aberration ( $P < .001$ ) in the high myopia group. The surgically induced amount of both coma and spherical aberration was significantly related to the amount of refractive correction ( $R=0.43$  and  $P < .001$  for coma;  $R=0.36$  and  $P < .01$  for spherical aberration). In the astigmatism group, there was a decrease, although not statistically significant, in the mean RMS of coma and spherical aberrations ( $P > .05$ ) over the smaller pupil size. The low myopia group exhibited no significant changes in the RMS values of midperipheral and peripheral high order aberrations over a 4-mm pupil after surgery ( $P > .05$ ), whereas the RMS error values of the combinations of terms with higher angular frequency (ie, midperipheral and peripheral high order aberrations) were significantly

increased in the high myopia ( $P < .05$ ) and astigmatism groups ( $P < .05$ ) over the smaller pupil diameter.

Coma-like aberration increased in all of the study groups over a 6-mm pupil size; however, the increase was statistically significant only in the two spherical ablation groups ( $P < .05$ ) and it was significantly related to the amount of refractive correction ( $R=0.42$  and  $P < .01$ ) (Fig 1). With pupil dilation, a large and significant increase in spherical aberration ( $P < .001$ ) was observed in both spherical myopia groups compared to the preoperative state, with a greater increase for deeper ablations (Fig 2). The postoperative spherical aberration was not statistically different ( $P > .05$ ) compared with the preoperative state in the astigmatism group over the larger pupil size. The combinations of terms having high angular frequency were not significantly increased after spherical myopic ablations ( $P > .05$ ). On the other hand, the surgically induced increase in mid-

peripheral ( $P<.05$ ) and peripheral ( $P<.05$ ) high order aberrations was statistically significant in the astigmatism group over a dilated pupil. Further, the increase in midperipheral and peripheral high order aberrations was significantly related to the amount of cylinder correction ( $R=-0.57$  and  $P<.05$  for midperipheral high order aberrations;  $R=-0.47$  and  $P<.05$  for peripheral high order aberrations) (Fig 3).

Corneal PSFs then were evaluated for each study group by averaging the effect of high order aberrations on the imaging performance of the first optical surface of the cornea, as specified in detail in a previous work.<sup>40</sup> The postoperative increased contribution of spherical aberration to overall high order wavefront aberration decreased the optical quality of the anterior corneal optics following simple myopic PRK, especially for deeper ablations (Fig 4), whereas following astigmatic correction, the optical image quality of the anterior cornea was mainly affected by the increased contribution of peripheral asymmetrical high order aberrations to overall high order corneal wavefront aberration.

### DISCUSSION

In an effort to optimize visual performance following procedures designed to reduce optical aberrations of the eye, a great deal of work has been carried out on how laser refractive surgery can modify both the distribution and contribution of specific high order terms to the overall high order wavefront aberration and the effect of their combinations on vision function.<sup>13,14,16,41,42</sup> Studies have demonstrated that each high order Zernike mode influences visual performance differently and that high order aberrations can interact specifically to improve acuity despite the increase in total wavefront error.<sup>15-17</sup> It has been suggested that minimizing the aberrations near the center of the Zernike pyramid may improve visual performance after refractive procedure. Besides the role of the eye optics on image formation,<sup>15-17</sup> this phenomenon may be related to the Stiles-Crawford effect,<sup>43</sup> which causes the retina to have a less effective response to the peripheral portions of the aberrant incident wavefront. The Stiles-Crawford effect may have an additional retinal basis in the optical behavior of cone photoreceptors with a differential sensitivity of the cones to light from different points in the pupil.<sup>44-46</sup> However, less attention has been paid to the combination of Zernike terms having higher angular frequency, especially when the total RMS is relatively low.

To determine whether peripheral corneal high order aberrations may affect the optical image quality of the anterior cornea following PRK, we developed a power

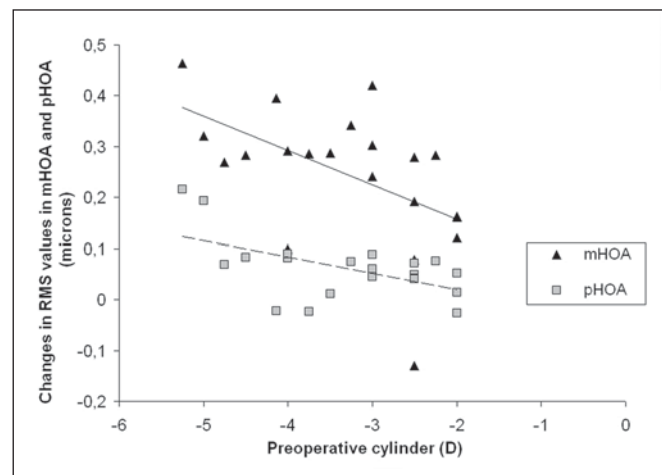


**Figure 3.** Scattergram of the surgically induced changes in root-mean-square (RMS) values in midperipheral (mHOA) and peripheral (pHOA) high order aberrations independent of the preoperative cylinder over a 6-mm pupil in the astigmatism group (Spearman correlation coefficients for midperipheral and peripheral high order aberrations were  $R=-0.57$  and  $R=-0.47$ , respectively, and  $P<.05$  for both). The increase in midperipheral and peripheral high order aberrations was related linearly to the amount of cylinder correction. The solid and dashed lines represent linear fits to the midperipheral and peripheral high order aberration values, respectively.

software tool that allowed us to separately analyze the weight and effect of specific combinations of Zernike high order terms having the same sign and angular frequency over two pupil diameters (4 mm and 6 mm) to characterize the optical image quality of the anterior cornea in different light conditions.

Previous works have shown that PRK changes the relative contribution of individual high order aberrations to the overall wavefront aberration and that the magnitude of the high order aberrations greatly increases with the attempted correction as well as pupil dilation.<sup>33,47-50</sup> Our findings agreed with previous results on the increase of high order aberrations following standard myopic laser correction. Preoperatively, aberrations were relatively low and dominated by coma-like aberration in all of the study groups over the smaller pupil size; following surface ablation, the magnitude of the corneal first surface wavefront aberration was increased within the optical zone, and the distribution of determined combinations of high order aberrations varied according to the amount of spherical equivalent treated and the ablation profile.

We noted the positive spherical aberration value increased significantly following the spherical treatments even within the central 4-mm pupil diameter. In a previous work, Hersh et al<sup>51</sup> hypothesized changes of corneal asphericity within the ablation zone could be related to the effect of corneal convexity on the ef-

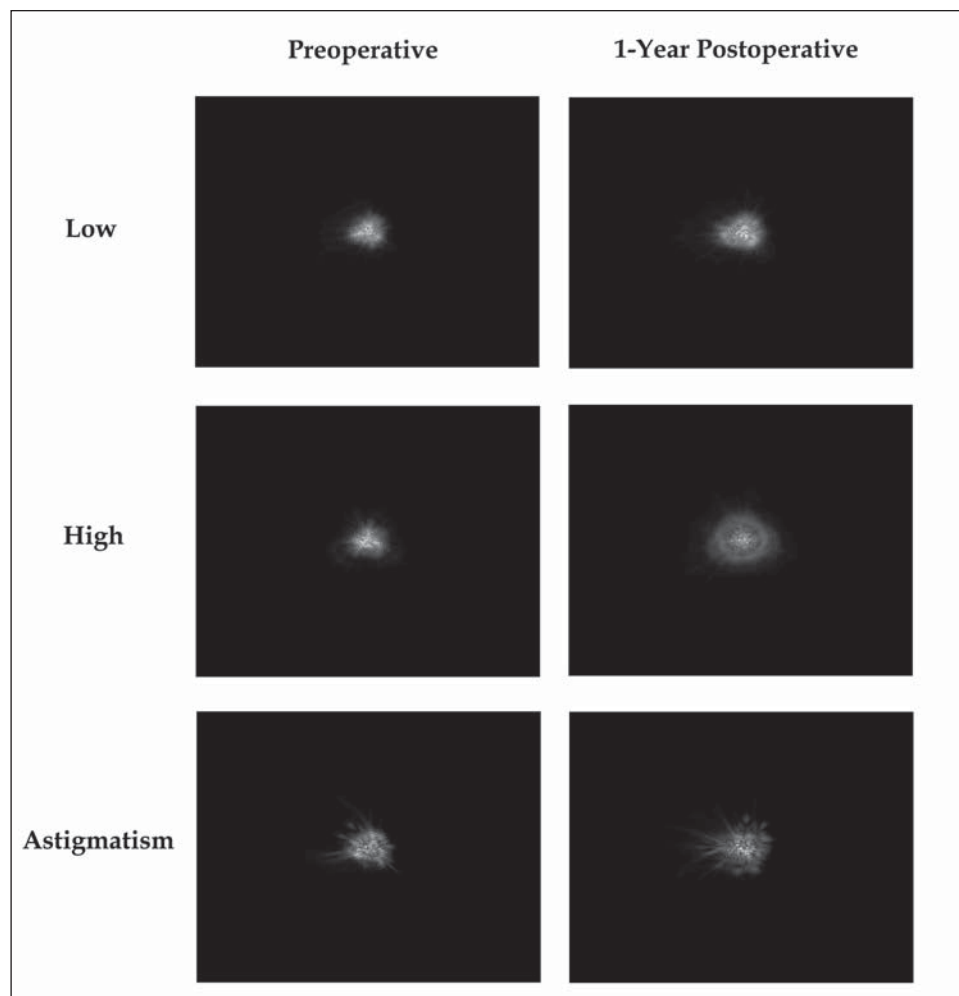


**Figure 4.** Average point spread function was computed from the high order corneal aberrations for a 6-mm pupil. Point spread functions subtend to a visual angle of 60' arc minutes. Postoperatively, the effect of anterior corneal spherical aberration increased in the low and high myopia groups, mainly for deeper ablations. Astigmatic correction increased the contribution of asymmetrical paracentral and peripheral high order aberrations to overall high order corneal wavefront aberration.

fective fluence of the incoming laser beam and hence the resulting decrease in peripheral fluence may be the cause for unforeseen underablation of the peripheral treatment zone with a consequent oblate result. In addition, Marcos et al<sup>52</sup> stated the increase in spherical aberration for the central 4 mm of the cornea after myopic ablation was not due to the ablation profile and parameters but possibly to biomechanical and healing effects; nevertheless, ablation algorithms are proprietary, and we cannot correctly simulate them.<sup>53</sup> On the other hand, the cross-cylinder technique did not deeply modify spherical aberration, probably due to the flattening of the corneal periphery induced by photorefractive astigmatic keratectomy ablation.<sup>54</sup>

Over a dilated pupil, spherical-like aberration dominated the high order aberration structure after simple myopic ablations, whereas peripheral asymmetrical aberrations were predominant following cylindrical treatment. The contribution of combinations of terms having higher angular frequency (ie, midperipheral and peripheral high order aberrations) to the overall high order wavefront aberration over the smaller pupil

size was significantly increased by either the deeper spherical myopic and cylindrical ablations, whereas after pupil dilation, peripheral aberrations were found to significantly change only with cylindrical corrections. Low myopia treatment did not appear to influence the quality of peripheral corneal optics. These results may be related primarily to the alignment of ablation on the pupillary axis, which is decentered with respect to the corneal reference axis,<sup>55</sup> and to the asymmetric biomechanical response between the nasal and temporal meridians of the cornea to photoablation, which has been shown to be positively related both to the amount of tissue removed as well as to larger treatment zones.<sup>56</sup> Hence, the greater impact of peripheral high order aberrations on the overall high order corneal wavefront in comparison with paracentral high order aberrations following cylindrical ablation may result from the more peripheral ablation of photorefractive astigmatic keratectomy and then from the different biomechanical properties of the periphery of the corneal plane, as stated previously.<sup>56</sup>

The PSF was more practical than the normalized

Zernike expansion to show the quality of the corneal optics<sup>36,37</sup> because of the complex interaction between modes at low levels of optical error.<sup>9,21,36,37</sup> In this work, we confirmed that deeper myopic ablations have a greater impact on the image quality formation of the central corneal optics and showed that the more peripheral the ablation, the more the image quality of peripheral corneal optics worsened. Further work is required to understand the effect of the complex interactions of individual terms on visual performance in both natural and treated eyes. Nevertheless, weighting the effect of interactions between all of the possible combinations of Zernike terms on visual performance may be too complicated to realistically achieve.

Our data cannot be extrapolated for LASIK or other excimer laser systems in which the effect of the flap creation and the proprietary ablation profile and parameters may have different influences on the corneal remodeling and the related biomechanical and optical responses of the cornea.<sup>40,56</sup> Limitations of our work include the fact that we did not consider internal wavefront aberrations. It is widely held that wavefront-guided procedures should always take the corneal front surface and the total wavefront aberrations into consideration.<sup>12,28,57,58</sup> Hence, full knowledge of the preoperative corneal topography as well as of the ocular high order aberration pattern and its impact on visual performance would be necessary for designing an ideal compensating algorithm for the individual cornea to maximize the quality of the whole eye optics, especially in eyes with large pupils. An accurate spherocylindrical correction combined with an additional midperipheral ablation to optimize the asphericity of the postoperative corneal profile<sup>59</sup> and minimize the regional asymmetries of the cornea<sup>56</sup> may improve future advanced ablations.

#### REFERENCES

1. Thibos LN. The prospects for perfect vision. *J Refract Surg.* 2000;16:S540-S546.
2. Applegate RA, Thibos LN, Hilmantel G. Optics of aberroscopy and super vision. *J Cataract Refract Surg.* 2001;27:1093-1107.
3. Nagy ZZ, Palagyi-Deak I, Kelemen E, Kovacs A. Wavefront-guided photorefractive keratectomy for myopia and myopic astigmatism. *J Refract Surg.* 2002;18:S615-S619.
4. Thibos LN, Bradley A, Hong X. A statistical model of the aberration structure of normal, well-corrected eyes. *Ophthalmic Physiol Opt.* 2002;22:427-433.
5. Wang Y, Zhao K, Jin Y, Niu Y, Zuo T. Changes of higher order aberration with various pupil sizes in the myopic eye. *J Refract Surg.* 2003;19:S270-S274.
6. Roberts C. Future challenges to aberration-free ablative procedures. *J Refract Surg.* 2000;16:S623-S629.
7. Phusitphoykai N, Tungsiripat T, Siriboonkoom J, Vongthongsri A. Comparison of conventional versus wavefront-guided laser in situ keratomileusis in the same patient. *J Refract Surg.* 2003;19:S217-S220.
8. Mrochen M, Bueeler M, Iseli HP, Hafezi F, Seiler T. Transferring wavefront measurements into corneal ablations: an overview of related topics. *J Refract Surg.* 2004;20:S550-S554.
9. Smolek MK, Klyce SD. Zernike polynomial fitting fails to represent all visually significant corneal aberrations. *Invest Ophthalmol Vis Sci.* 2003;44:4676-4681.
10. Tutt R, Bradley A, Begley C, Thibos LN. Optical and visual impact of tear break-up in human eyes. *Invest Ophthalmol Vis Sci.* 2000;41:4117-4123.
11. He JC, Burns SA, Marcos S. Monochromatic aberrations in the accommodated human eye. *Vision Res.* 2000;40:41-48.
12. Artal P, Guirao A, Berrio E, Williams DR. Compensation of corneal aberrations by the internal optics in the human eye. *J Vis.* 2001;1:1-8.
13. Thibos LN. Are higher order wavefront aberrations a moving target unworthy of clinical treatment? *J Refract Surg.* 2002;18:744-745.
14. Williams D, Yoon GY, Porter J, Guirao A, Hofer H, Cox I. Visual benefit of correcting higher order aberrations of the eye. *J Refract Surg.* 2000;16:S554-S559.
15. Applegate RA, Sarver EJ, Khemsara V. Are all aberrations equal? *J Refract Surg.* 2002;18:S556-S562.
16. Applegate RA, Marsack JD, Ramos R, Sarver EJ. Interaction between aberrations to improve or reduce visual performance. *J Cataract Refract Surg.* 2003;29:1487-1495.
17. Applegate RA, Ballentine C, Gross H, Sarver EJ, Sarver CA. Visual acuity as a function of Zernike mode and level of root mean square error. *Optom Vis Sci.* 2003;80:97-105.
18. Steinert R. The theoretical effect of measured wavefront diameter on estimating peripheral wavefront data. *J Refract Surg.* 2004;20:S597-S600.
19. Seo KY, Lee JB, Kang JJ, Lee ES, Kim EK. Comparison of higher-order aberrations after LASEK with a 6.0 mm ablation zone and a 6.5 mm ablation zone with blend zone. *J Cataract Refract Surg.* 2004;30:653-657.
20. Wang L, Koch DD. Ocular higher-order aberrations in individuals screened for refractive surgery. *J Cataract Refract Surg.* 2003;29:1896-1903.
21. Cheng X, Thibos LN, Bradley A. Estimating visual quality from wavefront aberration measurements. *J Refract Surg.* 2003;19:S579-S584.
22. Koch DD, Kohnen T, Obstbaum SA, Rosen ES. Format for reporting refractive surgical data. *J Cataract Refract Surg.* 1998;24:285-287.
23. Vinciguerra P, Sborgia M, Epstein D, Azzolini M, MacRae S. Photorefractive keratectomy to correct myopic or hyperopic astigmatism with a cross-cylinder ablation. *J Refract Surg.* 1999;15:S183-S185.
24. Serrao S, Lombardo M. One-year results of photorefractive keratectomy with and without surface smoothing using the Technolas 217C laser. *J Refract Surg.* 2004;20:444-449.
25. Gobbe M, Guillon M, Maissa C. Measurement repeatability of corneal aberrations. *J Refract Surg.* 2002;18:S567-S571.
26. Born M, Wolf E. *Principles of Optics.* 1st ed. New York, NY: Pergamon Press; 1959.
27. Mahajan VN. Zernike circle polynomials and optical aberrations of systems with circular pupil. *Applied Optics.* 1994;33:8121-8124.
28. Marcos S, Barbero S, Llorente L, Merayo-Llodes J. Optical response to LASIK surgery for myopia from total and corneal aber-



- ration measurements. *Invest Ophthalmol Vis Sci.* 2001;42:3349-3356.
29. Iskander DR, Collins MJ, Davis B. Optimal modeling of corneal surfaces with Zernike polynomials. *IEEE Trans Biomed Eng.* 2001;48:87-95.
  30. Thibos LN, Applegate RA, Schwiegerling JT, Webb R; VSIA Standards Taskforce Members. Standards for reporting the optical aberrations of eyes. *J Refract Surg.* 2002;18:S652-S660.
  31. Thibos LN. Wavefront data reporting and terminology. *J Refract Surg.* 2001;17:S578-S583.
  32. Wang L, Dai E, Koch DD, Nathoo A. Optical aberrations of the human anterior cornea. *J Cataract Refract Surg.* 2003;29:1514-1521.
  33. Oshika T, Klyce SD, Applegate RA, Howland HC, El Danasoury MA. Comparison of corneal wavefront aberrations after photorefractive keratectomy and laser in situ keratomileusis. *Am J Ophthalmol.* 1999;127:1-7.
  34. Seiler T, Kaemmerer M, Mierdel P, Krinke HE. Ocular optical aberrations after photorefractive keratectomy for myopia and myopic astigmatism. *Arch Ophthalmol.* 2000;118:17-21.
  35. Campbell CE. A new method for describing the aberrations of the eye using Zernike polynomials. *Optom Vis Sci.* 2003;80:79-83.
  36. Campbell CE. Improving visual function diagnostic metrics with the use of higher-order aberration information from the eye. *J Refract Surg.* 2004;20:S495-S503.
  37. Marsack JD, Thibos LN, Applegate RA. Metrics of optical quality derived from wave aberrations predict visual performance. *J Vis.* 2004;4:322-328.
  38. Castejon-Mochon JF, Lopez-Gil N, Benito A, Artal P. Ocular wave-front aberration statistics in a normal young population. *Vision Res.* 2002;42:1611-1617.
  39. Cheng X, Bradley A, Hong X, Thibos LN. Relationship between refractive error and monochromatic aberrations of the eye. *Optom Vis Sci.* 2003;1:43-49.
  40. Lombardo M, Lombardo G, Serrao S. Interocular high-order corneal wavefront aberration symmetry. *J Opt Soc Am A Opt Image Sci Vis.* 2006;23:777-787.
  41. Marcos S. Aberrations and visual performance following standard laser vision correction. *J Refract Surg.* 2001;17:S596-S601.
  42. Applegate RA, Hilmantel G, Howland HC, Tu EY, Starck T, Zayac J. Corneal first surface optical aberrations and visual performance. *J Refract Surg.* 2000;16:507-514.
  43. Marcos S, Burns SA. On the symmetry between eyes of wavefront aberration and cone directionality. *Vision Res.* 2000;40:2437-2447.
  44. Burns SA, Wu S, Delori F, Elsner AE. Direct measurement of human-cone-photoreceptor alignment. *J Opt Soc Am A Opt Image Sci Vis.* 1995;12:2329-2338.
  45. Applegate RA, Lakshminarayanan V. Parametric representation of Stiles-Crawford functions: normal variation of peak location and directionality. *J Opt Soc Am A Opt Image Sci Vis.* 1993;10:1611-1623.
  46. Atchison DA, Joblin A, Smith G. Influence of Stiles-Crawford effect apodization on spatial visual performance. *J Opt Soc Am A Opt Image Sci Vis.* 1998;15:2545-2551.
  47. Martinez CE, Applegate RA, Klyce SD, McDonald MB, Medina JP, Howland HC. Effect of pupillary dilation on corneal optical aberrations after photorefractive keratectomy. *Arch Ophthalmol.* 1998;116:1053-1062.
  48. Oshika T, Miyata K, Tokunaga T, Samejima T, Amano S, Tanaka S, Hirohara Y, Mihashi T, Maeda N, Fujikado T. Higher order wavefront aberrations of cornea and magnitude of refractive correction in laser in situ keratomileusis. *Ophthalmology.* 2002;109:1154-1158.
  49. Anera RG, Jimenez JR, Jimenez del Barco L, Bermudez J, Hita E. Changes in corneal asphericity after laser in situ keratomileusis. *J Cataract Refract Surg.* 2003;29:762-768.
  50. Oliver KM, Hemenger RP, Corbett MC, O'Brart DP, Verma S, Marshall J, Tomlinson A. Corneal optical aberrations induced by photorefractive keratectomy. *J Refract Surg.* 1997;13:246-254.
  51. Hersh PS, Fry K, Blaker JW. Spherical aberration after laser in situ keratomileusis and photorefractive keratectomy. Clinical results and theoretical models of etiology. *J Cataract Refract Surg.* 2003;29:2096-2104.
  52. Marcos S, Cano D, Barbero S. Increase in corneal asphericity after standard laser in situ keratomileusis for myopia is not inherent to the Munnerlyn algorithm. *J Refract Surg.* 2003;19: S592-S595.
  53. Gatinel D, Hoang-Xuan T, Azar DT. Determination of corneal asphericity after myopia surgery with the excimer laser: a mathematical model. *Invest Ophthalmol Vis Sci.* 2001;42:1736-1742.
  54. Schwiegerling J, Snyder RW. Corneal ablation patterns to correct for spherical aberration in photorefractive keratectomy. *J Cataract Refract Surg.* 2000;26:214-221.
  55. Bueeler M, Mrochen M, Seiler T. Maximum permissible torsional misalignment in aberration-sensing and wavefront-guided corneal ablation. *J Cataract Refract Surg.* 2004;30:17-25.
  56. Serrao S, Lombardo G, Lombardo M. Differences in nasal and temporal responses of the cornea after photorefractive keratectomy. *J Cataract Refract Surg.* 2005;31:30-38.
  57. Mrochen M, Jankov M, Bueeler M, Seiler T. Correlation between corneal and total wavefront aberrations in myopic eyes. *J Refract Surg.* 2003;19:104-112.
  58. Atchison DA. Anterior corneal and internal contributions to peripheral aberrations of human eyes. *J Opt Soc Am A Opt Image Sci Vis.* 2004;21:355-359.
  59. Yoon G, MacRae S, Williams DR, Cox IG. Causes of spherical aberration induced by laser refractive surgery. *J Cataract Refract Surg.* 2005;31:127-135.